Organic Electronics 13 (2012) 1081–1085

Contents lists available at SciVerse ScienceDirect

Organic Electronics

journal homepage: www.elsevier.com/locate/orgel

# Outcoupling efficiency of organic light emitting diodes employing graphene as the anode

Sei-Yong Kim [a], Jang-Joo Kim [b,*]

[a] Department of Materials Science and Engineering and Center for Organic Light Emitting Diode, Seoul National University, Seoul 151-742, South Korea
[b] WCU Hybrid Materials Program, Department of Materials Science and Engineering and Center for Organic Light Emitting Diode, Seoul National University, Seoul 151-742, South Korea

ARTICLE INFO

*Article history:*
Received 26 November 2011
Received in revised form 14 February 2012
Accepted 19 February 2012
Available online 14 March 2012

*Keywords:*
Outcoupling efficiency
Graphene anode
OLEDs
Transparent electrode

ABSTRACT

Outcoupling efficiencies (OCEs) of green phosphorescent organic light emitting diodes (OLEDs) with graphene anodes are theoretically analyzed using the classical electromagnetic model and are compared with the OLEDs with ITO anodes. The OCEs of the OLEDs with anodes of 3 or 4 graphene monolayers are comparable to an ITO based device with a 150 nm thick ITO, where both electrodes have a similar sheet resistance of about 24 Ω/□. However, the OCEs of graphene based OLEDs are lower than that for ITO based devices with a same sheet resistance in most cases. This limitation can be overcome by using a graphene/transparent conducting oxide (ITO or IZO) composite electrode, which can achieve high outcoupling efficiency, low sheet resistance and high transmittance at the same time. In addition to that, the light extraction techniques are expected to be much more effective in graphene based OLEDs than ITO based OLEDs, which is important for lighting application of OLEDs.



## 1. Introduction

In recent years, the organic light emitting diodes (OLEDs) industry has expanded their focus to large area and flexible displays, beyond the display for smart phones. Unfortunately, ITO, the most commonly used transparent conducting electrode, is difficult to use as an electrode for large area flexible displays because ITO is brittle and easily generates cracks under bending stress [1,2]. Moreover, ITO is a major factor in rising costs, due to a depletion of resources and an increase in the complexity of the fabrication process for the device. For these reasons, graphene has received great attention to replace ITO. Graphene is a material possessing high conductivity, high charge mobility and high transmittance (~97.7% per monolayer) in the entire visible range [3–5]. Furthermore, graphene shows a high stretchability as well as the chemical and thermal stability [3,6]. Thus, graphene has been applied to various optoelectronic devices [3,6–12]. In OLEDs, graphene has been used as a transparent electrode or injection buffer between the organic layer and the ITO [9–11]. However, graphene based OLEDs showed low efficiency compared to ITO based OLEDs. High contact resistance (~hundreds Ω/□) [10,12] and a lack of optical analysis about an optimum device structure are the major causes of the low performance. There is a theoretical prediction of the outcoupling efficiency (OCE) of a graphene based OLED with a fixed structure to show a similar OCE with an ITO based control device [10]. Since the optimum device structure giving the highest outcoupling efficiency depends on the thickness and refractive index of the transparent electrodes (TE) [13], the simple replacement of the transparent electrode with fixed organic layer thicknesses is insufficient to interpret the outcoupling efficiency for graphene based OLEDs.

In this paper, we analyzed the OCEs of green phophorescent OLEDs with graphene as the anode using the classical electromagnetic model and compared it with ITO based devices. We systematically varied the thickness of

* Corresponding author.
*E-mail address:* jjkim@snu.ac.kr (J.-J. Kim).

1566-1199/$ - see front matter © 2012 Elsevier B.V. All rights reserved.
http://dx.doi.org/10.1016/j.orgel.2012.02.018

the organic layers and the location of the emission zone (EZ) with the thicknesses of the graphene and ITO layer as the parameters. To obtain meaningful results, the OCEs were plotted as a function of the sheet resistance of the transparent electrodes. The maximum OCEs of the OLED with 3 or 4 monolayers of graphene as the anode (24%) are comparable with a device with 150 nm thick ITO (25%), where the sheet resistances are almost the same between the electrodes with 24 Ω/□. However, the OCEs of graphene based OLEDs are lower than the ITO based devices with the same sheet resistance in most cases. This limitation of lower OCEs in graphite based OLEDs compared to ITO based ones can be overcome by the graphene/transparent conducting oxides (ITO or IZO) composite electrode. Calculation results predict that the graphene/ITO or IZO composite layer has a large potential to get a high OCE with a low sheet resistance and high outcoupling efficiency at the same time.

## 2. Brief description about theoretical approach

The OLEDs used for the calculation of the OCE have a layered structure consisting of a thick reflective cathode, an organic layer, a transparent electrode layer and semi-infinite glass as shown in Fig. 1. Graphene, ITO or ITO/graphene composite electrode was used as the transparent anode. The *N,N′*-dicarbazolyl-4-4′-biphenyl (CBP) layer doped with 6 wt.% *N,N′*-dicarbazolyl-3,5-benzene (mCP) and *fac*-tris(2-phenylpyridine) iridium ($Ir(ppy)_3$) was considered as the organic layer. We simplified the multiple organic layers to a single emitting layer because the refractive indices of the organic semiconductors commonly used in the devices are not significantly different. For simplicity, the dipole radiators are embedded in the layered structure as a sheet and their orientations are randomly distributed. The sheet dipole approximation is not the limitation of this calculation because any distribution of excitons in a real device can be easily accounted for by the weighted integration of the calculated OCEs based on the sheet dipole approximation. The intrinsic photo-luminescent (PL) quantum yields of the phosphorescent dyes are assumed to be 100% in the simulation, which is reasonable for $Ir(ppy)_3$ [14,15]. The classical electromagnetic model, which considers an exciton as a radiating dipole, is applied for the purpose of optical modeling in OLEDs. The detailed procedure and formulation of the optical modeling have been described before [13,15–17]. The complex refractive indices (RI) of graphene and the organic material were obtained from the reported literature [13,18]. The optical constants of glass, ITO and Al were also obtained from the literature [19,20]. In the optical modeling, the thickness of the multilayer graphene (X in Fig. 1) is assumed to be $nt_{mono}$, where $n$ is the number of monolayers and $t_{mono}$ is the thickness of the graphene monolayer (0.335 nm) [18]. The optical constants of graphene are assumed to be independent of the number of monolayers and the dependence on the fabrication condition of the graphene layer is ignored.

## 3. Results and discussion

The calculation results of the OCEs of the graphene based OLEDs are displayed in Fig. 2. The outcoupling efficiency of the ITO based OLEDs for the selective thicknesses of ITO (80, 150 and 270 nm, respectively) are also plotted in Fig. 2 for comparison. We calculated the OCEs for a number of monolayers up to 10. The simulation results show that the maximum OCE for the 1st mode of the graphene OLEDs is 0.243, which is significantly lower than the maximum OCE of 0.304 for the ITO based OLEDs which is achieved with an ITO thickness of 80 nm. However, when we compare this with an OLED with an ITO thickness of 150 nm, which is commonly used in practical OLEDs in order to have a low enough sheet resistance, the OCEs of the graphene based OLEDs are almost the same as the ITO based OLEDs. It is interesting to note that the thickness

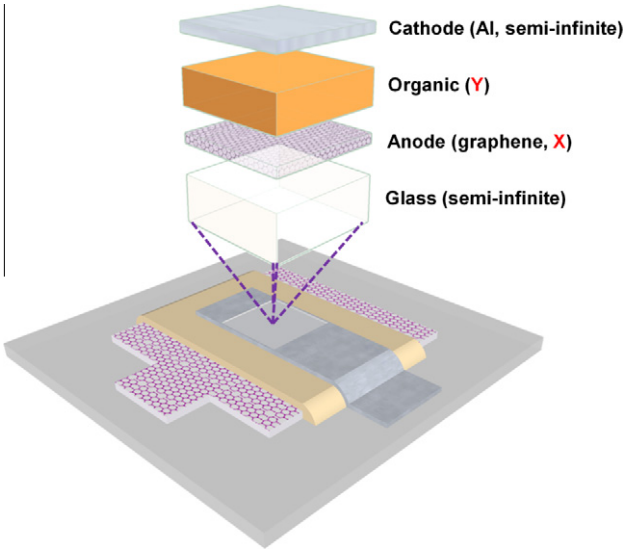


**Fig. 1.** Schematic diagram of the device structure used in optical modeling. X and Y indicate the thickness of graphene and organic layer, respectively.

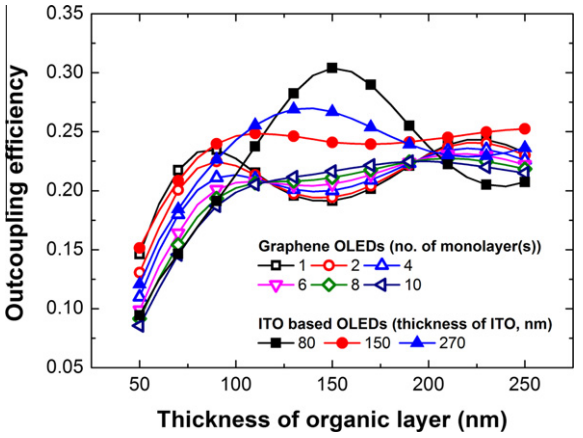


**Fig. 2.** The calculation results of the maximum OCEs for the graphene based OLEDs with a number of graphene monolayers up to 10 (open polygon) and the OCEs of ITO based OLEDs (closed polygons) for selective thicknesses of ITO (80, 150, and 270 nm, respectively).

of the organic layer at the 1st anti-node, giving the largest OCE, is much thinner (90–100 nm) than for the ITO based OLEDs (150 nm) when the number of the graphene monolayers are less than 6. This difference comes from the different phase changes of the emitted light between the thin graphene layer and the thicker ITO layer.

Although the OCEs of graphene based OLEDs are lower than ITO based devices, as shown in Fig. 2, it would be more informative to compare the maximum achievable OCEs against the sheet resistance of the electrodes because the sheet resistance is an important parameter for current driving devices such as OLEDs. The sheet resistance of graphene was calculated using the following equation [10];

$$R_s = \frac{1}{\sigma_{2D} N} \tag{1}$$

where $R_s$ is the sheet resistance, $\sigma_{2D}$ is the bidimensional conductivity described by $n\mu e$ (where $n$, $\mu$ and $e$ are the density of charge carrier, the mobility of carrier and the unit charge, respectively.), and $N$ is the number of graphene monolayers. Two limiting values for the mobility and carrier density of $\mu = 2.0 \times 10^3\ \mathrm{cm^2/V\,s}$ and $n = 1.0 \times 10^{13}/\mathrm{cm^3}$, and of $\mu = 2.0 \times 10^4\ \mathrm{cm^2/V\,s}$ and $n = 3.4 \times 10^{12}/\mathrm{cm^3}$ were used for the calculation of the sheet resistance of graphene [7,10]. The calculation results of the thickness vs. sheet resistance are plotted in Fig. 3a. The experimental data of the sheet resistance for various thicknesses of graphene and ITO referred from the literature are plotted in Fig. 3a [21,22]. Fig. 3a shows that the recent experimental data of doped and pristine graphene are well matched with two theoretical limitations up to 4 monolayers. To achieve a sheet resistance of 10 Ω/□, only 3.35 nm of graphene (for $\mu = 2.0 \times 10^4\ \mathrm{cm^2/V\,s}$ and $n = 3.4 \times 10^{12}/\mathrm{cm^3}$) are needed while the thickness of the ITO should be larger than 250 nm. The maximum OCEs achievable at given thicknesses of the graphene and ITO electrodes are plotted against the sheet resistance in Fig. 3b. The maximum OCE of the ITO based OLEDs is about 30% when the ITO thickness is around 80 nm. However, the sheet resistance of the 80 nm thick ITO is 70 Ω/□, which is not practical to use as an anode for OLEDs. Thus, the thickness of the ITO should be increased to reduce the sheet resistance. For this reason, 150 nm thick ITO is most widely used as the anode of OLEDs where their sheet resistance becomes around 20 Ω/□. Thicker ITO can reduce the sheet resistance further but at the expense of the transmittance and for a higher price. The OCE is 0.252 of the OLEDs with a 150 nm thick ITO layer whose sheet resistance is 23 Ω/□. The OCE of the graphene based OLEDs having a similar sheet resistance is about 0.240 for $\mu = 2.0 \times 10^4\ \mathrm{cm^2/V\,s}$ and $n = 3.4 \times 10^{12}/\mathrm{cm^3}$, which is comparable to the OCE of the ITO based OLED. This is an encouraging result illustrating the possibility that the graphene based OLEDs can achieve a similar performance to an ITO based device. With an exception around 150 nm thick ITO, however, the OCEs of the graphene based OLEDs are still lower than the ITO based devices. The lower OCEs of the graphene based OLEDs originate from the low reflectance of the graphene layer resulting in a weak interference effect from the weak microcavity structure.

This limitation of a lower OCE in graphite based OLEDs can be overcome by the use of a graphene/Indium Zinc Oxide (IZO) composite electrode. By using a composite of a graphene layer and an IZO layer we can achieve high conductivity, high transparency and flexibility at the same time. IZO is a transparent conducting oxide which can be deposited at room temperature and possesses flexibility because its structure is amorphous [2]. Unfortunately IZO has a higher sheet resistance than ITO. By forming a composite electrode of IZO and graphene, we can take advantages of both materials to get low sheet resistance and high flexibility. Furthermore, the IZO plays a role of a weak mirror or phase changing layer to enhance the internal interference effect resulting in high OCE through controlling their thickness. The schematic diagram of the device structure used in the calculation is illustrated in Fig. 3c. The refractive index of IZO is assumed to be the same as for ITO [20,23]. The number of graphene layers for the composite electrode is fixed to 4 where the transmittance and the sheet resistance of the graphene layer become similar to that for 150 nm thick ITO (~90% transmittance and 20–30 Ω/□ sheet resistance). The sheet resistance of the composite electrode was calculated from the known sheet resistance of IZO [23] and graphene using the following formula evaluated from the transmission line model (TLM) for bi-layer structure, ignoring the contact resistance between the graphene and the IZO film [24].

$$R_{sh,composite} = \frac{R_{sh,graphene} R_{sh,IZO}}{R_{sh,graphene} + R_{sh,IZO}} \tag{2}$$

where $R_{sh,composite}$ is the sheet resistance of the composite electrode and $R_{sh,grapheneorIZO}$ is the sheet resistance of graphene or IZO, respectively. The calculation results of the maximum OCEs are included in Fig. 3b. The sheet resistance of the graphene composite is located below 20 Ω/□ even with the 40 nm thick IZO layer, while the 190 nm thick ITO layer is required to get the sheet resistance, demonstrating that the composite electrodes can realize low

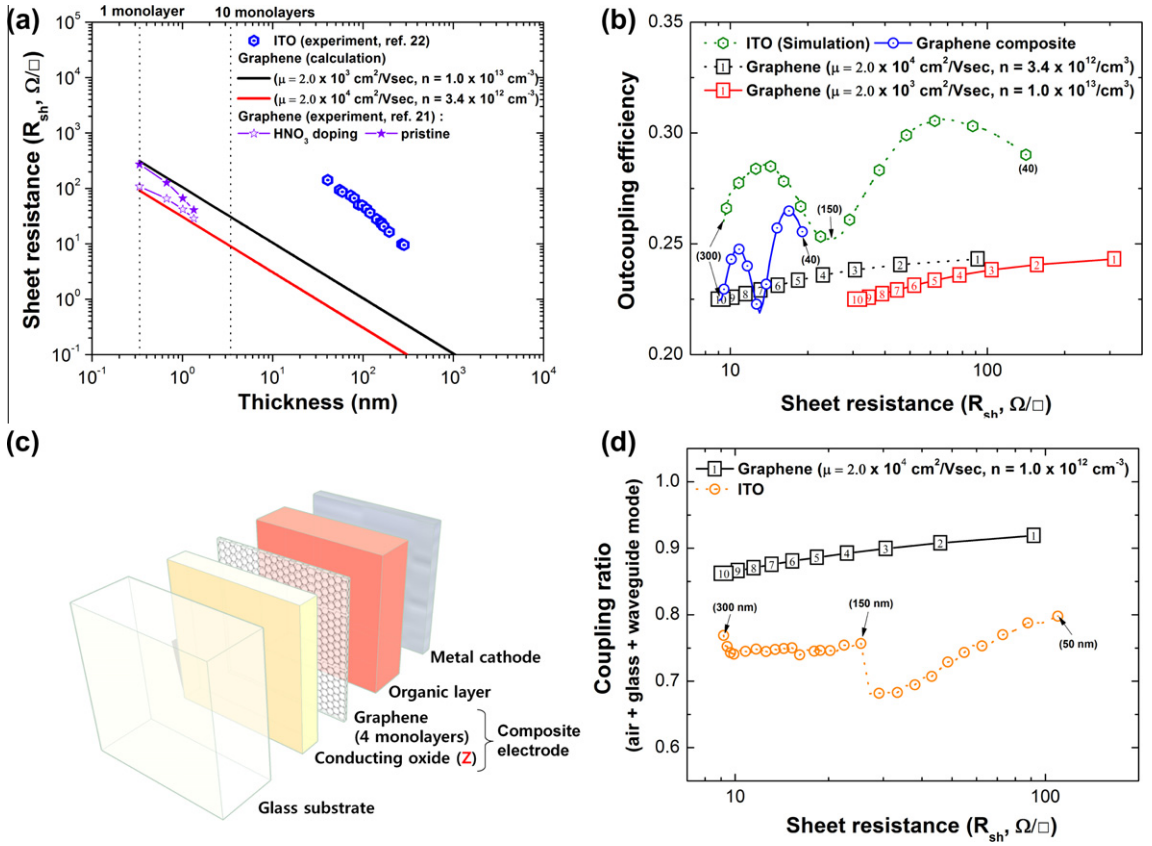


**Fig. 3.** (a) The calculation results of the thickness vs. sheet resistance. Two limiting values for the mobility and carrier density $\mu = 2.0 \times 10^3$ cm$^2$/V $s$ and $n = 1.0 \times 10^{13}$ cm$^3$ for the black solid line, and $\mu = 2.0 \times 10^4$ cm$^2$/V $s$ and $n = 3.4 \times 10^{12}$/ cm$^3$ for the red solid line) are selected for calculation of the sheet resistance. The scatters indicate the experimental results of ITO (blue hexagons) and graphene (open and closed stars for $HNO_3$ doped and undoped graphene, respectively) from literature. (b) The calculation results of the OCEs against the sheet resistance of graphene, ITO and composite based devices. The numbers indicate the thickness of ITO or IZO (inside the brackets) and number of graphene monolayer(s) (inside of the squares), respectively. (c) The schematic diagram of the device structure with graphene composite used for simulation. Z indicates the thickness of the IZO layer of the composite electrode, which is varied from 40 (19 Ω/□) to 300 nm (9.5 Ω/□). The thickness of the organic layer (X in Fig. 1) was also varied. (d) The calculation results of the coupling ratio consisting of radiation, glass confined and waveguide mode for graphene and ITO based OLEDs. The numbers in Fig. 3d are the same meaning as those in Fig. 3b (For interpretation of the references to color in this figure legend, the reader is referred to the web version of this article.).

sheet resistance results very easily. The OLEDs with the composite electrode composed of 4 monolayer graphene/80 nm thick IZO can obtain the maximum OCE of 0.265 at 16.9 Ω/□ which is higher than the OLEDs with the graphene only electrode or with the 150 nm thick ITO electrode, while the sheet resistance of the composite electrode is much lower than that of the other electrodes, demonstrating the potential of the composite electrode with a low sheet resistance and high outcoupling efficiency compared with ITO based OLEDs. Although we predicted the enhancement of the OCEs by using the composite electrode, the OCEs of the graphene based OLEDs are still lower than the ITO based OLEDs in the wide range of sheet resistance.

The situation changes if we consider the incorporation of light extraction layers in OLEDs which is getting more popular for lighting application of OLEDs [25–28]. In such cases, ultimate limit of the total extracted light is the summation of the air mode, glass confined mode and waveguide mode in the electrode and organic layers. The calculation results are displayed in Fig. 3d. The graphene based OLEDs show much higher ultimate outcoupling ratio than ITO based OLEDs in the entire range of sheet resistance. Therefore, the light extraction techniques are expected to be much more effective in graphene based OLEDs than ITO based OLEDs.

## 4. Conclusion

We theoretically analyzed the OCEs of green phosphorescent OLEDs with graphene as the anode using the classical electromagnetic model. The OCEs of the OLEDs with 3 and 4 monolayers of graphene as the anode are comparable to the ITO based device with the 150 nm thick ITO, where both electrodes have a similar sheet resistance of about 24 Ω/□. However, the OCEs of graphene based OLEDs are lower than the ITO based devices with the same sheet resistance in most cases. This limitation can be overcome by the graphene/ITO (or IZO) composite electrode, which can achieve high outcoupling efficiency, low sheet resistance and high transmittance at the same time. The OLED with the 4 monolayer graphene/80 nm thick IZO

composite electrodes can obtain the maximum OCE of 0.265 at 16.9 Ω/□, which is higher than the OLEDs with the graphene only electrode or the 150 nm thick ITO electrode, while the sheet resistance of the composite electrode is much lower than that of the other electrodes. Although IZO (or ITO) was used as a component of the graphene composite electrode, indium free conducting oxide such as aluminum doped zinc oxide (AlZnO) can be used instead of IZO. The graphene based OLEDs show much higher ultimate outcoupling ratio including the air mode, glass confined mode and waveguide mode than ITO based OLEDs in the entire range of sheet resistance. Therefore, the light extraction techniques are expected to be much more effective in graphene based OLEDs than ITO based OLEDs, which is important for lighting application of OLEDs.

## Acknowledgements

This work was supported by the Industrial strategic technology development program [10035225, Development of core technology for high performance AMOLED on plastic] funded by MKE/KEIT of Korea.

## References

[1] M. Boehme, C. Charton, Properties of ITO on PET film in dependence on the coating conditions and thermal processing, Surf. Coat. Technol. 200 (2005) 932–935.
[2] J.W. Kang, W.I. Jeong, J.J. Kim, H.K. Kim, D.G. Kim, G.H. Lee, High-performance flexible organic light-emitting diodes using amorphous indium zinc oxide anode, Electrochem. Solid State 10 (6) (2007) J75–J78.
[3] X. Wang, L. Zhi, K. Mullen, Transparent, conductive graphene electrodes for dye-sensitized solar cells, Nano Lett. 8 (2008) 323–327.
[4] K.I. Bolotin, K.J. Sikes, Z. Jiang, M. Klima, G. Fudenberg, J. Hone, P. Kim, H.L. Stormer, Ultrahigh electron mobility in suspended graphene, Solid State Commun. 146 (2008) 351–355.
[5] A.B. Kuzmenko, E. van Heumen, F. Carbone, D. van der Marel, Universal optical conductance of graphite, Phys. Rev. Lett. 100 (2008) 117401.
[6] D.I. Son, T.W. Kim, J.H. Shim, J.H. Jung, D.U. Lee, J.M. Lee, W.I. Park, W.K. Choi, Flexible organic bistable devices based on graphene embedded in an insulating poly(methyl methacrylate) polymer layer, Nano Lett. 10 (2010) 2441–2447.
[7] F. Bonaccorso, Z. Sun, T. Hasan, A.C. Ferrari, Graphene photonics and optoelectronics, Nat. Photonics 4 (2010) 611–622.
[8] X.L. Feng, S.P. Pang, Y. Hernandez, K. Mullen, Graphene as transparent electrode material for organic electronics, Adv. Mater. 23 (2011) 2779–2795.
[9] T. Sun, Z.L. Wang, Z.J. Shi, G.Z. Ran, W.J. Xu, Z.Y. Wang, Y.Z. Li, L. Dai, G.G. Qin, Multilayered graphene used as anode of organic light emitting devices, Appl. Phys. Lett. 96 (2010) 133301.
[10] J.B. Wu, M. Agrawal, H.A. Becerril, Z.N. Bao, Z.F. Liu, Y.S. Chen, P. Peumans, Organic light-emitting diodes on solution-processed graphene transparent electrodes, Acs Nano 4 (2010) 43–48.
[11] Z. Zhong, Y. Dai, D. Ma, Z.Y. Wang, Facile synthesis of organo-soluble surface-grafted all-single-layer graphene oxide as hole-injecting buffer material in organic light-emitting diodes, J. Mater. Chem. 21 (2011) 6040–6045.
[12] P. Blake, P.D. Brimicombe, R.R. Nair, T.J. Booth, D. Jiang, F. Schedin, L.A. Ponomarenko, S.V. Morozov, H.F. Gleeson, E.W. Hill, A.K. Geim, K.S. Novoselov, Graphene-based liquid crystal device, Nano Lett. 8 (2008) 1704–1708.
[13] S.-Y. Kim, J.J. Kim, Outcoupling efficiency of organic light emitting diodes and the effect of ITO thickness, Org. Electron. 11 (2010) 1010–1015.
[14] Y. Kawamura, K. Goushi, J. Brooks, J.J. Brown, H. Sasabe, C. Adachi, 100% phosphorescence quantum efficiency of Ir(III) complexes in organic semiconductor films, Appl. Phys. Lett. 86 (2005) 071104.
[15] W.I. Jeong, S.Y. Kim, J.W. Kang, J.J. Kim, Thickness dependence of PL efficiency of organic thin films, Chem. Phys. 355 (2009) 25–30.
[16] R.R. Chance, A. Prock, R. Silbey, Molecular Fluorescence and Energy Transfer Near Interfaces, John Wiley & Sons, Inc., 1978.
[17] J.A.E. Wasey, W.L. Barnes, Efficiency of spontaneous emission from planar microcavities, J. Mod. Opt. 47 (2000) 725–741.
[18] V.G. Kravets, A.N. Grigorenko, R.R. Nair, P. Blake, S. Anissimova, K.S. Novoselov, A.K. Geim, Spectroscopic ellipsometry of graphene and an exciton-shifted van Hove peak in absorption, Phys. Rev. B 81 (2010) 155413.
[19] E.D. Palik, G. Ghosh, Handbook of Optical Constants of Solids, Academic Press, San Diego, 1998.
[20] R.A. Synowicki, Spectroscopic ellipsometry characterization of indium tin oxide film microstructure and optical constants, Thin Solid Films 313 (1998) 394–397.
[21] S. Bae, H. Kim, Y. Lee, X.F. Xu, J.S. Park, Y. Zheng, J. Balakrishnan, T. Lei, H.R. Kim, Y.I. Song, Y.J. Kim, K.S. Kim, B. Ozyilmaz, J.H. Ahn, B.H. Hong, S. Iijima, Roll-to-roll production of 30-inch graphene films for transparent electrodes, Nat. Nanotechnol. 5 (2010) 574–578.
[22] D.H. Kim, M.R. Park, H.J. Lee, G.H. Lee, Thickness dependence of electrical properties of ITO film deposited on a plastic substrate by RF magnetron sputtering, Appl. Surf. Sci. 253 (2006) 409–411.
[23] S.T. Kim, J.H. Lee, J.Y. Yang, S.W. Ryu, J.S. Hong, W.P. Hong, J.-J. Kim, H.M. Kim, J.M. Yang, S.H. Park, The electronic and optical properties of IZO thin films prepared by pulsed DC magnetron sputtering, J. Korean Phys. Soc. 50 (2007) 662–665.
[24] G.K. Reeves, H.B. Harrison, Using TLM principles to determine MOSFET contact and parasitic resistance, Solid State Electron. 41 (1997) 1067–1074.
[25] Y. Sun, S.R. Forrest, Enhanced light out-coupling of organic light-emitting devices using embedded low-index grids, Nat. Photonics 2 (2008) 483–487.
[26] H.H. Cho, B. Park, H.-J. Kim, S. Jeon, J.H. Jeong, J.-J. Kim, Solution-processed photonic crystals to enhance the light outcoupling efficiency of organic light-emitting diodes, Appl. Opt. 49 (2010) 4024–4028.
[27] S. Jeon, J.W. Kang, H.D. Park, J.-J. Kim, J.R. Youn, J. Shim, J.H. Jeong, D.G. Choi, K.D. Kim, A.O. Altun, S.H. Kim, Y.H. Lee, Ultraviolet nanoimprinted polymer nanostructure for organic light emitting diode application, Appl. Phys. Lett. 92 (2008) 223307.
[28] H.H. Cho, B. Park, H.-J. Kim, J.Y. Shim, S. Jeon, J.-H. Jeong, J.-J. Kim, Planarization of nanopatterned substrates using solution process to enhance outcoupling efficiency of organic light emitting diodes, Curr. Appl. Phys. 10 (2010) e139–e142.